

Supporting Information

Efficient deep-blue electroluminescence with $\text{CIEy} \in (0.05\text{--}0.07)$ from phenanthroimidazole–acridine derivative hybrid fluorophores

Shuo Chen,^a Jiarong Lian,^a Weigao Wang,^b Yue Jiang,^a Xuedong Wang,^c Shuming Chen,^b Pengju Zeng,^{*,a} Zhengchun Peng^{*,a}

^a Key Laboratory of Optoelectronic Devices and Systems of Ministry of Education and Guangdong Province, College of Optoelectronic Engineering, Shenzhen University, Shenzhen, Guangdong, 518060, P.R. China

^b Department of Electrical and Electronic Engineering, Southern University of Science and Technology, Shenzhen, Guangdong, 518055, P. R. China

^c Key Laboratory for Carbon-Based Functional Materials and Devices Institute of Functional Nano and Soft Materials (FUNSOM) of Jiangsu Province, Soochow University, Suzhou, Jiangsu, 215123, P.R. China

*Email - zcpeng@szu.edu.cn

Index

	Content	Page No.
Figure S1	^1H NMR spectrum of compound PhImBr .	1
Figure S2	^1H NMR spectrum of compound PhImAc .	1
Figure S3	^1H NMR spectrum of compound PhImEn .	2
Figure S4	HR-MS spectrum of compound PhImBr .	2
Figure S5	HR-MS spectrum of compound PhImAc .	3
Figure S6	HR-MS spectrum of compound PhImEn .	3
Figure S7	Absorption spectra of PhImAc and PhImEn in neat film.	4
Figure S8	Solvatochromic shifts of PL spectra of PhImAc (a) and PhImEn (b).	4
Figure S9	Phosphorescence spectra of PhImAc and PhImEn at 77 K.	5
Figure S10	TGA and DSC thermograms of PhImAc and PhImEn	6
Figure S11	Cyclic voltammogram of compounds PhImAc and PhImEn in the anode scan.	7
Figure S12	Energy level diagrams of the WOLEDs C and D	8
Figure S13	Performance of WOLEDs C and D.	9

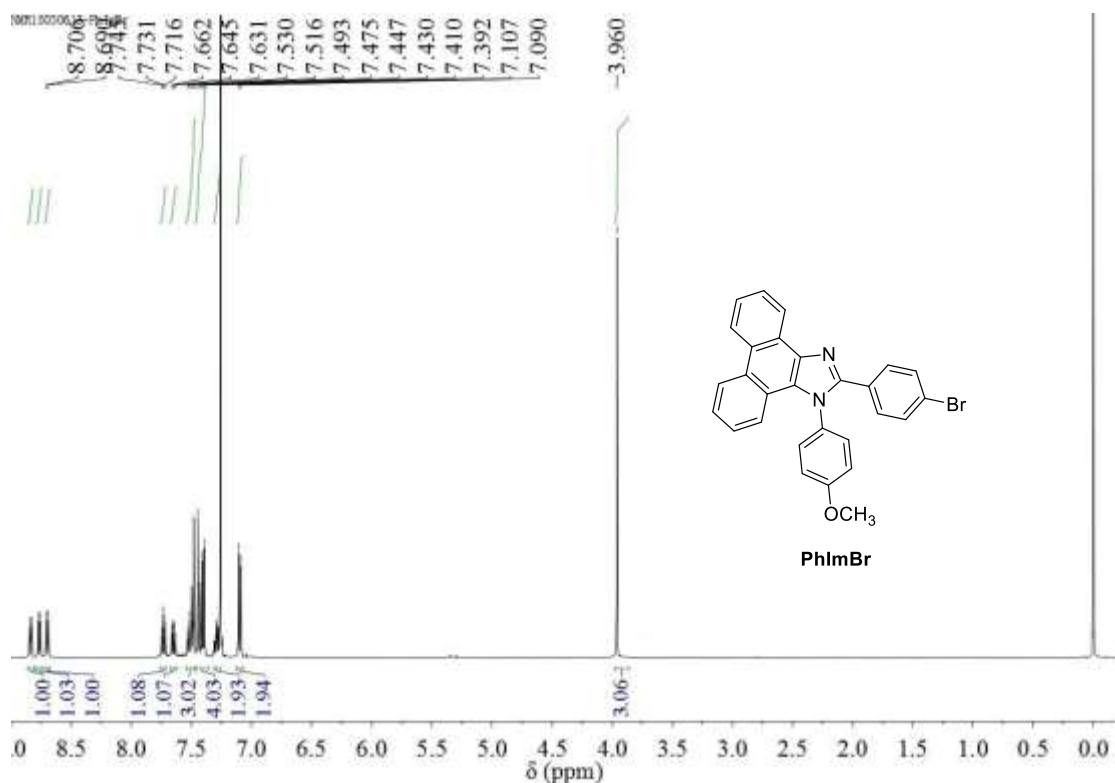


Figure S1. ¹H NMR spectrum of compound PhImBr.

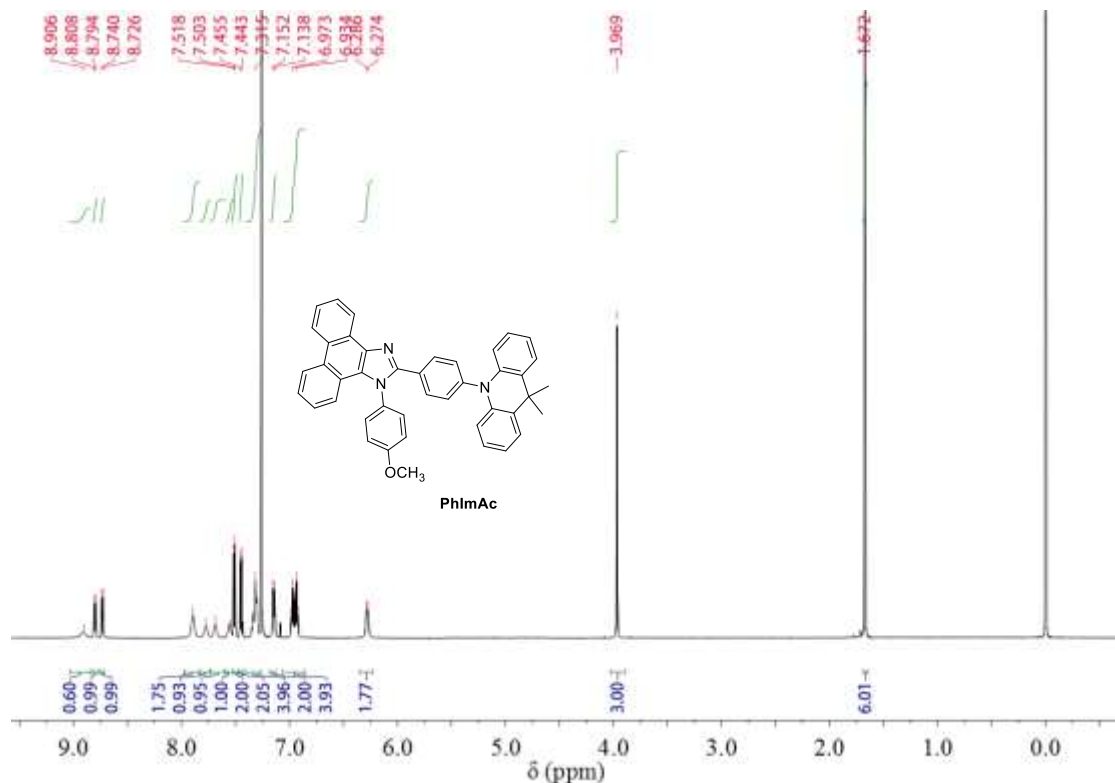


Figure S2. ¹H NMR spectrum of compound PhImAc.

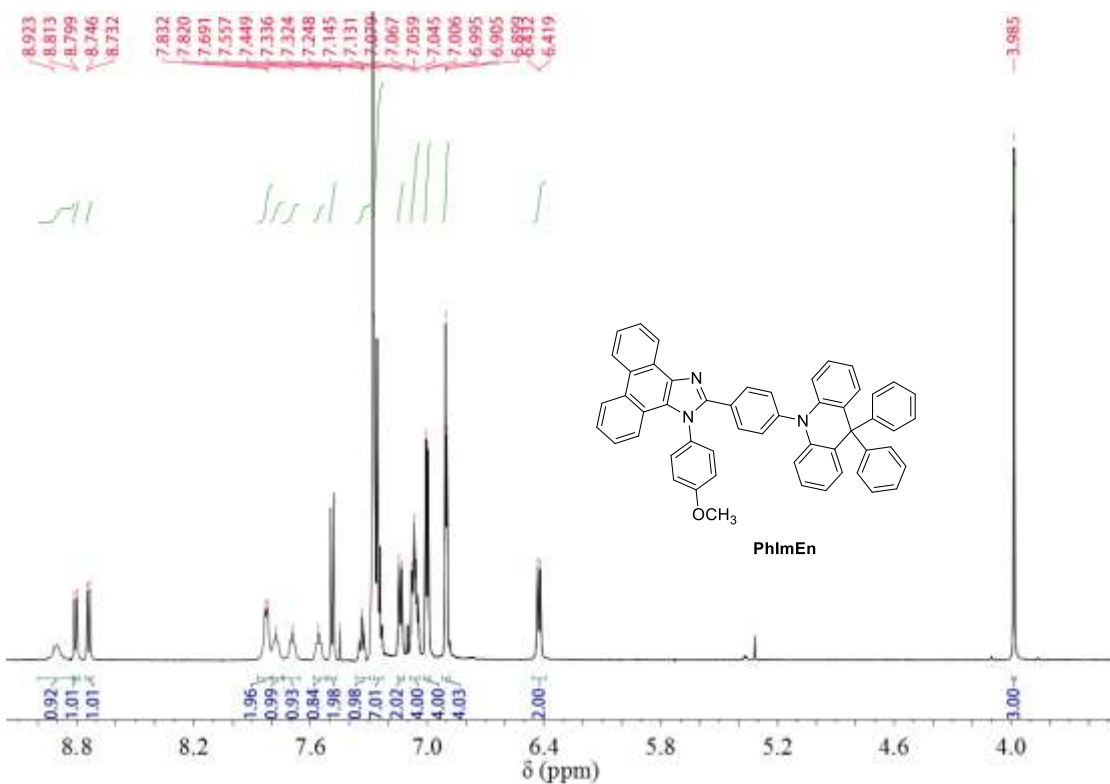


Figure S3. ^1H NMR spectrum of compound **PhImEn**.

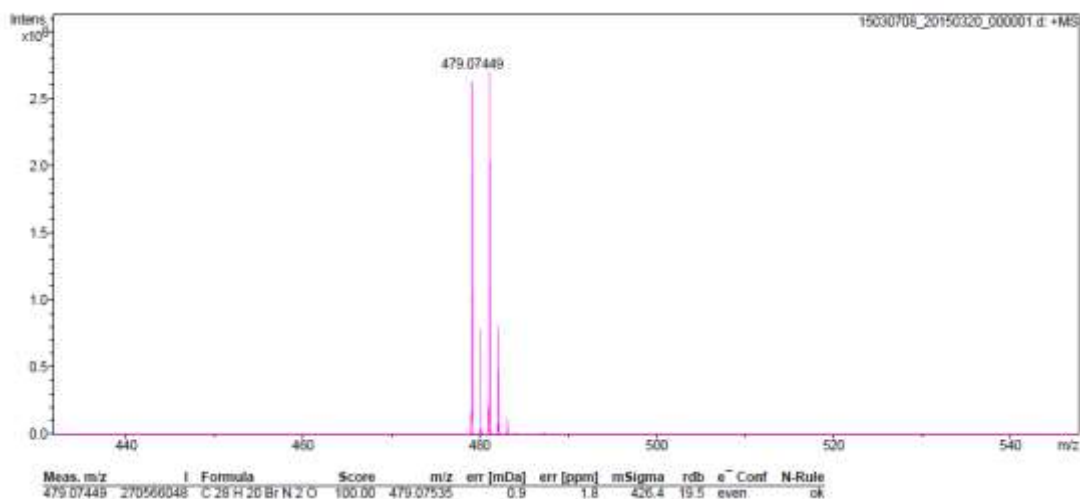


Figure S4. HR-MS spectrum of compound **PhImBr**.

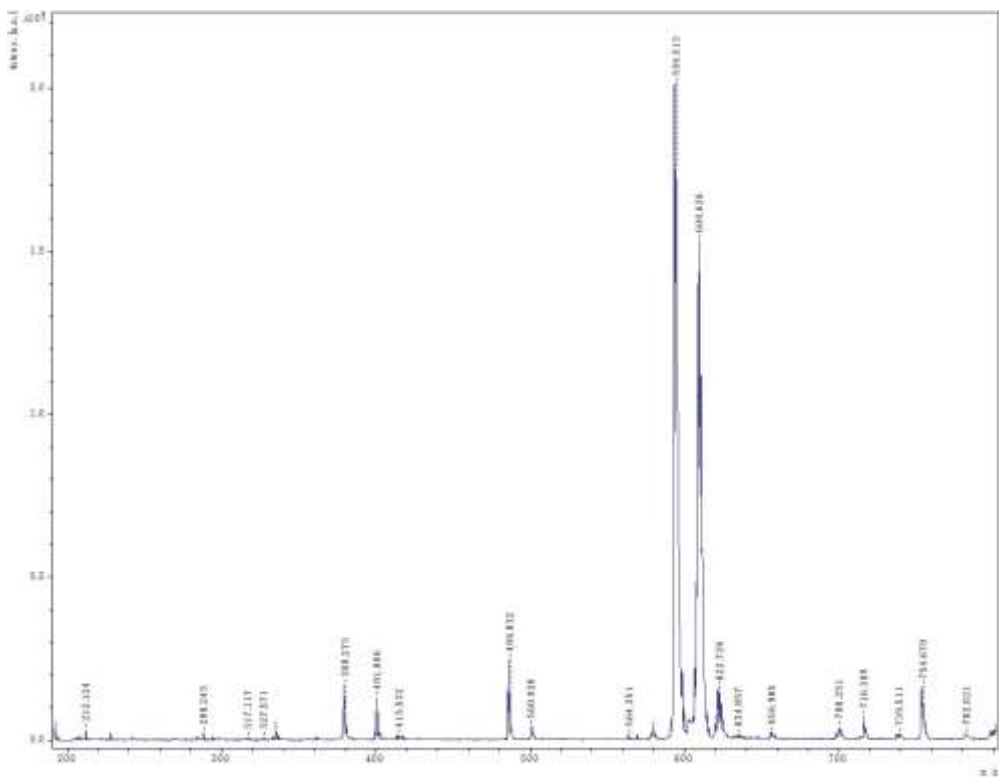


Figure S5. HR-MS spectrum of compound PhImAc.

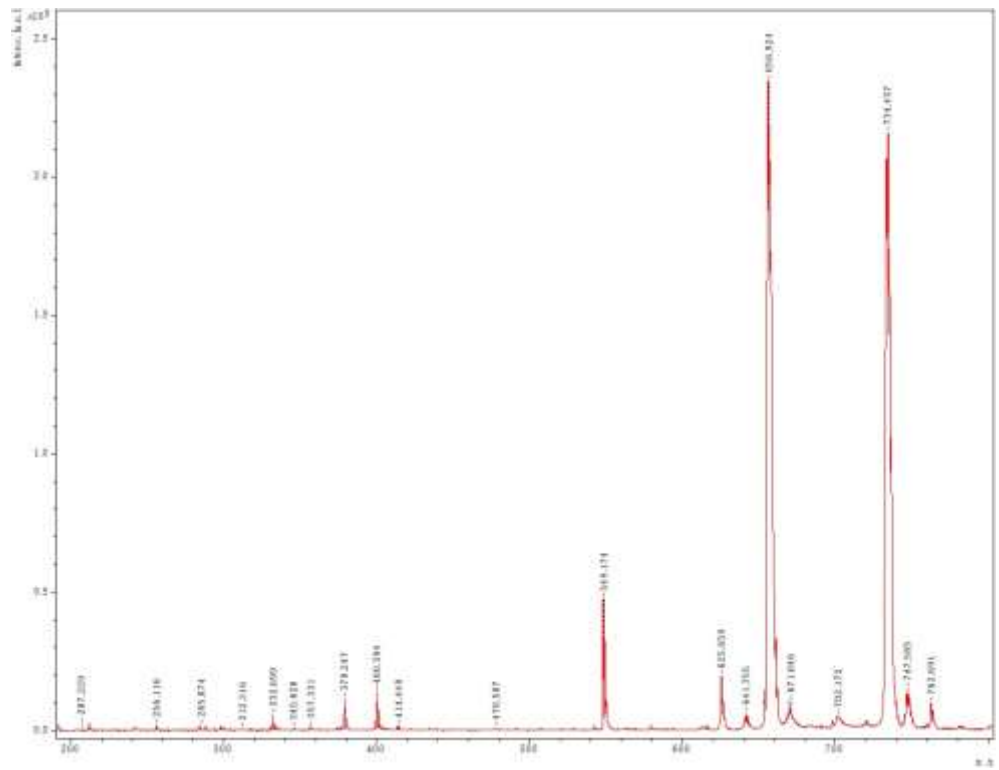


Figure S6. HR-MS spectrum of compound PhImEn.

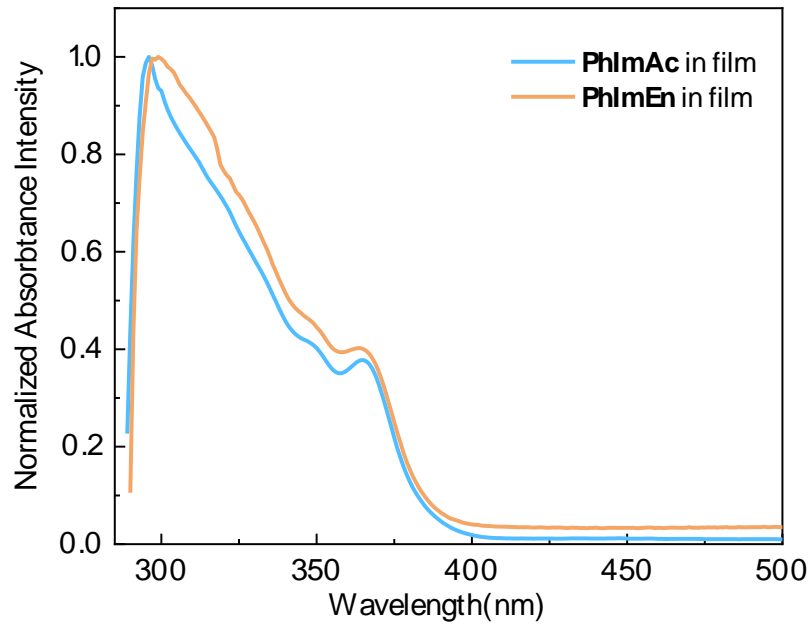


Figure S7. Stead-state absorption spectra of **PhImAc** and **PhImEn** in neat film at room temperature.

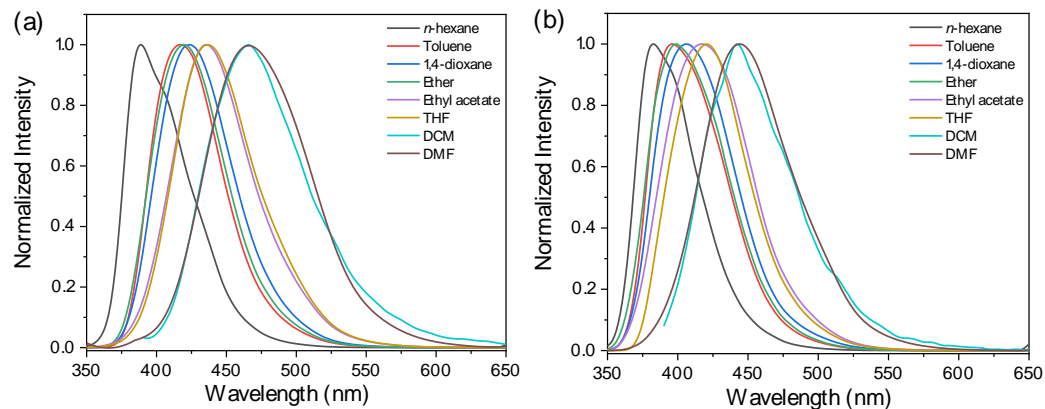


Figure S8. Solvatochromic shifts of PL spectra of **PhImAc** (a) and **PhImEn** (b).

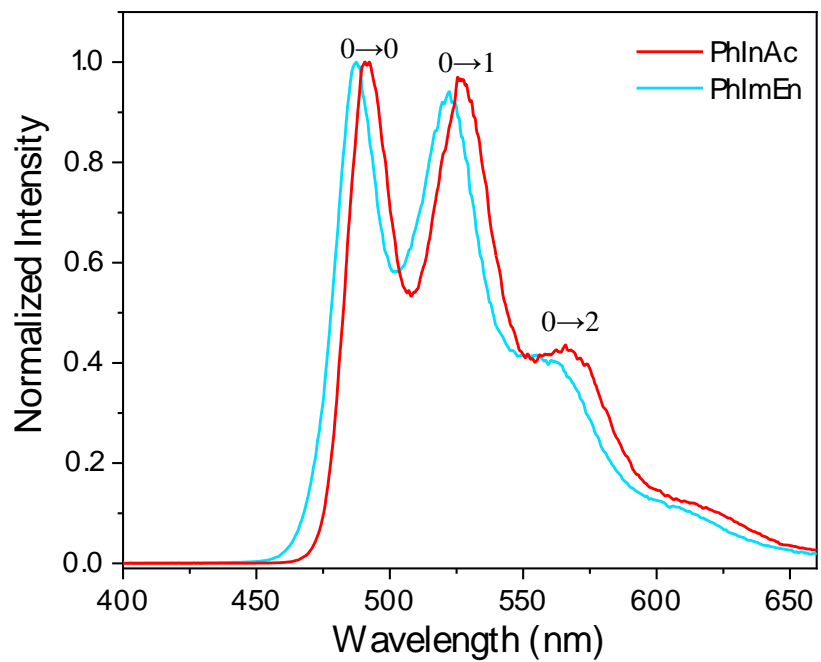


Figure S9. Phosphorescence spectra of **PhImAc** and **PhImEn** in toluene at 77 K.

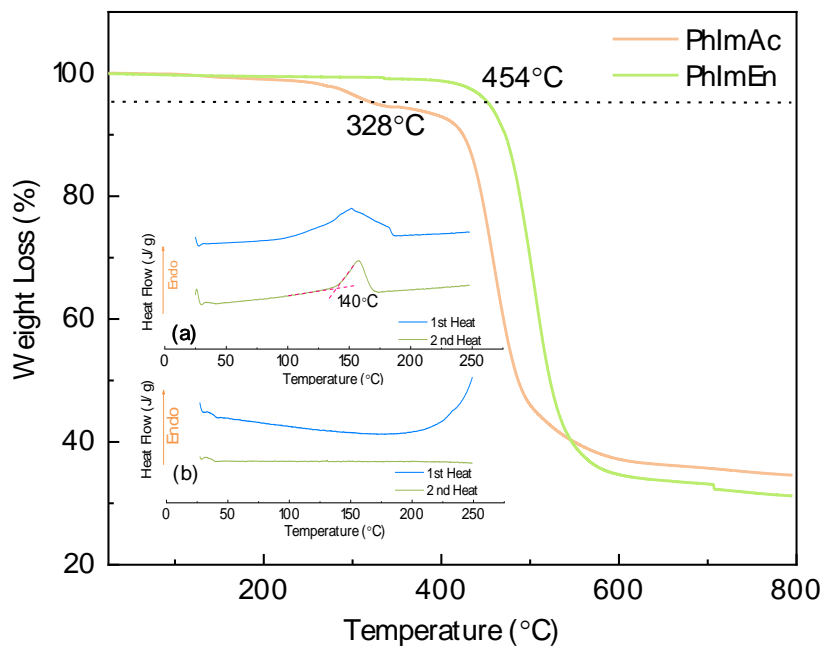


Figure S10. TGA thermograms of **PhImAc** and **PhImEn** measured at $10\text{ }^{\circ}\text{C min}^{-1}$ under nitrogen flushing. Insert: DSC spectra of the first and second heating cyclings for **PhImAc** (a) and **PhImEn** (b), at a heating rate of $10\text{ }^{\circ}\text{C min}^{-1}$ under nitrogen flushing.

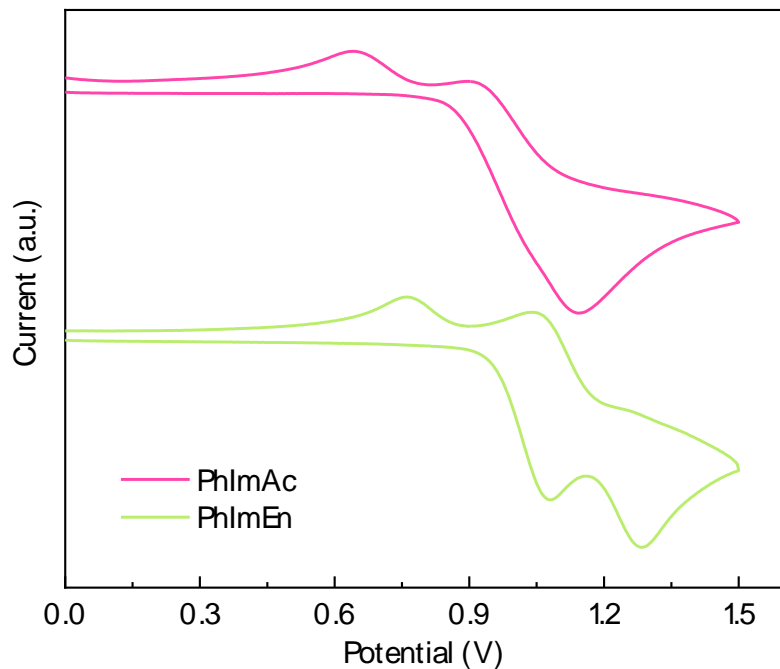


Figure S11. Cyclic voltammogram of compounds **PhImAc** and **PhImEn** in the anode scan.

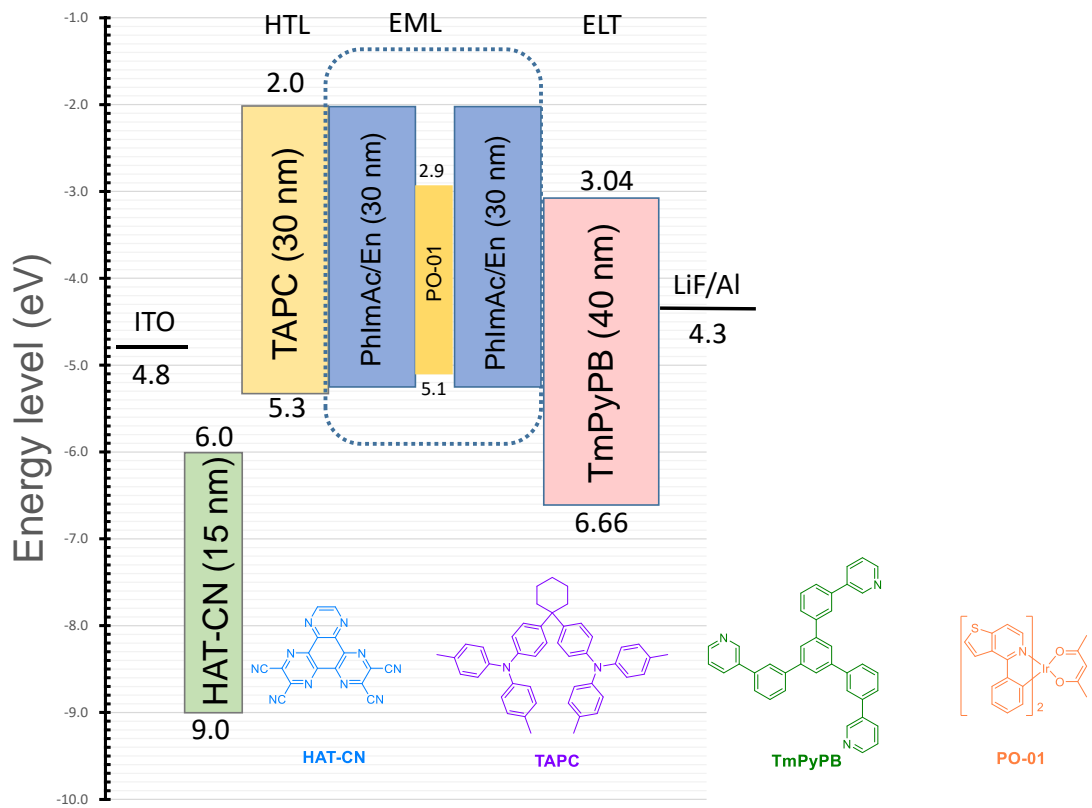


Figure 12. Energy level diagrams of the WOLEDs C and D based on **PhImAc** and **PhImEn** as host and PO-01 as dopant.

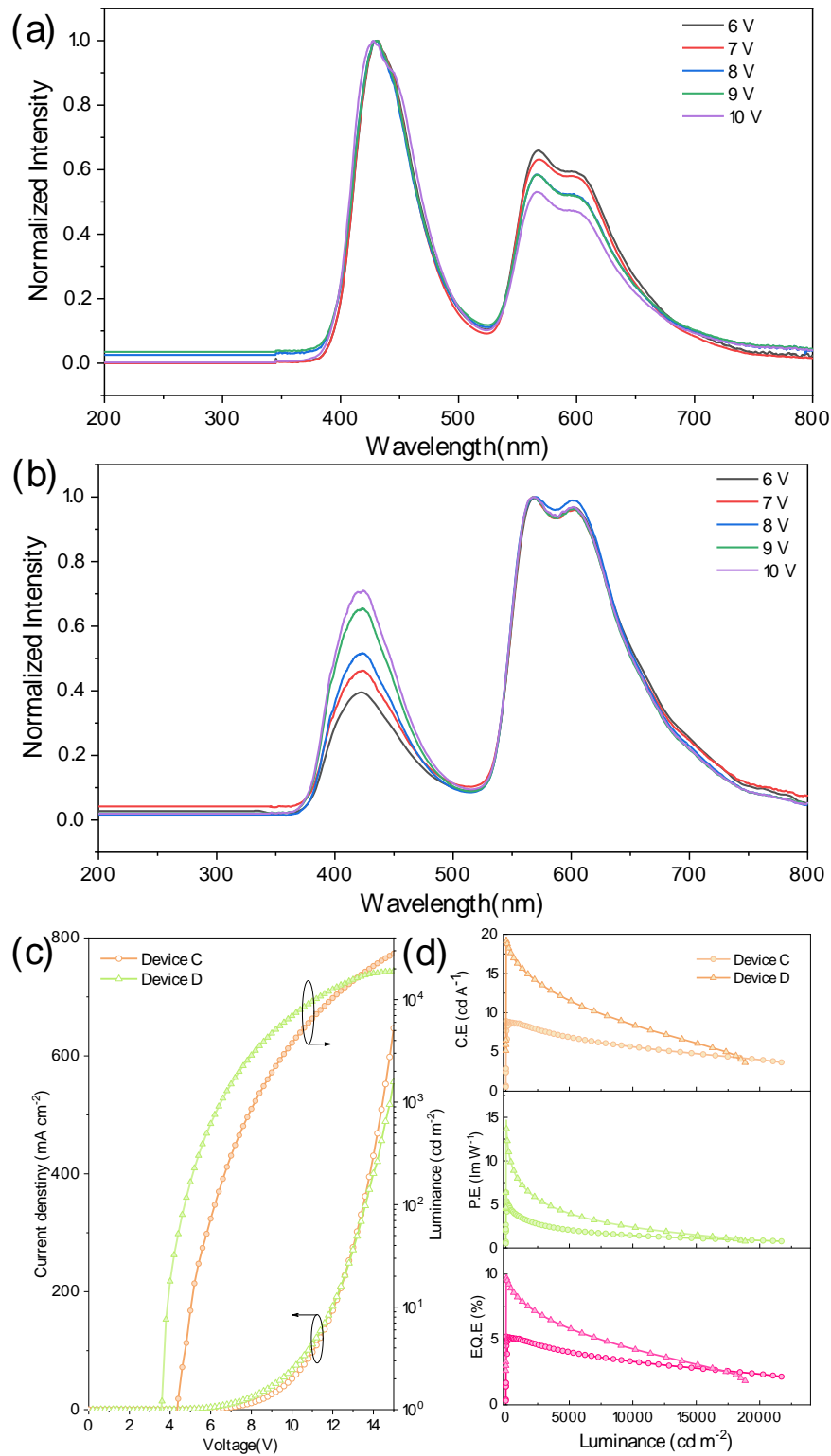


Figure S13. (a) Electroluminescence spectra for WOLED C. (b) Electroluminescence spectra for WOLED D at different voltages. (c) Current density–voltage–luminance characteristics. (d) Efficiency versus luminance curves.